SAKARYA ÜNİVERSİTESİ
FEN BİLİMLERİ ENSTİTÜSÜ DERGİSİ

Sakarya University Journal of Science
SAUJS

ISSN 1301-4048 | e-ISSN 2147-835X | Period Bimonthly | Founded: 1997 | Publisher Sakarya University | http://www.saujs.sakarya.edu.tr/

Title: Photoluminescence Investigation of Tb Doped Yb_2O_3 Phosphors Produced by Precipitation Method

Authors: Fatma UNAL

Recieved: 2021-03-11 21:51:02

Accepted: 2021-07-07 16:18:29

Article Type: Research Article

Volume: 25
Issue: 4
Month: August
Year: 2021
Pages: 1031-1036

How to cite
Fatma UNAL; (2021), Photoluminescence Investigation of Tb Doped Yb_2O_3 Phosphors Produced by Precipitation Method. Sakarya University Journal of Science, 25(4), 1031-1036, DOI: 10.16984/saufenbilder.895402
Access link
http://www.saujs.sakarya.edu.tr/en/pub/issue/64755/895402

Sakarya University Journal of Science 25(4), 1031-1036, 2021

Photoluminescence Investigation of Tb Doped Yb_2O_3 Phosphors Produced by Precipitation Method

Fatma UNAL*[1]

Abstract

In this study, un-doped and Tb doped ytterbium oxide (Yb_2O_3:Tb^{3+}) particles with different dopant rates (2, 4, 6 and 8 at. %) were produced by precipitation method, followed by subsequent calcination at 1000 °C for 2 h. The crystal structure of all particles was cubic Yb_2O_3 structure. The presence of Tb ion in Yb_2O_3 host structure was proved from the XRD peak shift results. The crystal structure expanded compared to un-doped Yb_2O_3 particles with doping, confirming calculated lattice parameter (LP) values. The LP, crystallite size (CS) and dislocation density values were in the range of 1.0428 – 1.0596 nm, 16 – 25 nm and 0.00189 – 0.00391 nm^{-2}, respectively. Only one sharp emission peak was observed at 506 nm corresponding to $^5D_4 – {}^7F_6$ transition (green emission) from photoluminescence (PL) spectra of the phosphor particles. The PL emission intensities were found to be strongly dependent on both CS and dopant rate. There was a positive correlation between increasing CS, decreasing lattice strain/dislocation density and PL intensity. Crystal defects decreased and PL intensity increased up to 6 at. % dopant rate.

Keywords: Terbium doped ytterbium oxide phosphors, photoluminescence emission, precipitation method, Williamson-Hall analysis

1. INTRODUCTION

Lanthanide oxides have unique and versatile physical and chemical properties such as high melting point, corrosion resistance, excellent thermal stability, high dielectric constant, mechanical strength, good protective behavior, luminescence, etc. [1-3]. Among the lanthanide oxides, ytterbium oxide (Yb_2O_3) particles exhibit extraordinary properties [4]. Correspondingly, they have many application areas such as high-temperature superconducting materials, colored glasses, technical ceramic, varistors, catalyst, electro-catalysis, solid-state laser, phosphor, stabilizer, optical fiber, solid oxide fuel cell, medical echo probe, imaging, scintillator and NIR photovoltaic up-converters [1-3, 5-13]. However, since its commercialized use in electronic devices is limited due to the high band gap (~5 eV) of Yb_2O_3, lanthanide dopant elements (such as La, Ho, Gd, Er, Eu etc.) were integrated into the Yb_2O_3 host structure [1, 2, 9-11, 13]. They can be synthesized by many methods such as electrospinning, sol-gel, hydrothermal method, spray pyrolysis, precipitation [2, 3, 5-8]. While there are limited number of publications on the production of lanthanide doped Yb_2O_3 particles [1, 9-11, 13], there is no comprehensive study on

* Corresponding author: fatmaunal@hitit.edu.tr
[1] Hitit University, Corum, Turkey.
ORCID: https://orcid.org/ 0000-0003-4476-2544

the synthesis and photoluminescence (PL) properties of Yb_2O_3:Tb^{3+} particles. Herein, the first study on the effects of dopant rate and crystallite size (CS) values on the PL properties of Yb_2O_3:Tb^{3+} particles was reported.

2. EXPERIMENTAL STUDY

Un-doped and Tb doped ytterbium oxide (Yb_2O_3:Tb^{3+}) particles with different dopant rates (2, 4, 6 and 8 at. %) were produced by precipitation method using analytical grade, 99.99% purity, ytterbium (III) nitrate hydrate ($Yb(NO_3)_3 \cdot xH_2O$) and terbium-nitrate-hydrate ($Tb(NO_3)_3 \cdot xH_2O$). For example, 300 ml of 0.1 M solution was prepared for each sample. 10.56 gr of Yb-nitrate and 0.207 g of Tb-nitrate salts were used in order to produce 2 at. % Tb doped Yb_2O_3 particles. After dissolving appropriate amounts of nitrate salts in ultrapure water, they were mixed for 15 min in ambient conditions. Afterwards, 1 M ammonium carbonate ($(NH_4)_2CO_3$) solution was slowly added to each solution till precipitation was completed. The solutions were stirred in a magnetic stirrer for 3 h. They were centrifuged at 5000 rpm for 5 min to collect precipitate, which were further washed several times with distilled water and once with ethanol. Dried particles at 80°C for 24 hours were subjected to calcination at 1000 °C for 2 hours in a furnace. Sample codes are shown in Table 1.

Table 1 Sample codes of all the particles

Sample code	Temperature (°C) / Time (h)	Dopant rate (at. %)
Yb_2O_3	1000 / 2	0
02Tb:Yb_2O_3		2
04Tb:Yb_2O_3		4
06Tb:Yb_2O_3		6
08Tb:Yb_2O_3		8

All particles were investigated by X-ray diffraction technique (XRD) in order to find out phase structure. Using the XRD broadening data, lattice parameter (LP) and crystallite size (CS) values were computed with Williamson–Hall (W–H) and Cohen-Wagner (C–W) methods, respectively [5, 14]. To characterize the microstructural parameter (lattice strain, dislocation density), average CS values were computed with W–H analysis integrated with uniform deformation model. The diffraction peak's broadenings were measured by Eq. 1.

$$\beta_{hkl} = [(\beta_{hkl})^2_{measured} - \beta^2_{(instrumental)}]^{1/2} \quad (1)$$

The CS values of particles were computed with W–H by Eq. 2,

$$\beta_{hkl} cos\theta = \frac{k\lambda}{D} + (4\varepsilon sin\theta) \quad (2)$$

where β_{hkl} is calculated correct broadening of the XRD diffraction peak, k is a constant (0.89), θ is diffraction angle, λ is X-ray Cu-K_α wavelength (1.5406 Å), D and ε are denoted by crystallite size and lattice strain, respectively. The dislocation density was calculated by Williamson-Smallman formalism [14] (Eq. 3):

$$\delta = \frac{1}{D^2} \quad (3)$$

where δ is dislocation density and D is crystallite size. Photoluminescence (PL) emission spectra of Tb doped particles were taken between 300 nm and 800 nm under 254 nm excitation at room temperature.

3. RESULTS AND DISCUSSION

3.1. Structural Analysis

XRD patterns of un-doped and Tb doped Yb_2O_3 particles are given in Fig 1. It was determined that all the produced particles had body centered cubic Yb_2O_3 crystalline phase with space group *Ia*-3 (JCPDS card no: 00-43-1037) and no impurity phase was detected in the particles.

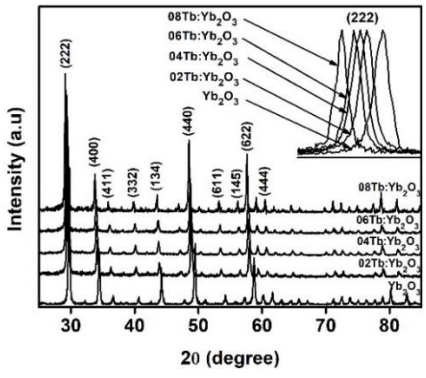

Figure 1 XRD patterns of all the particles

All diffraction peaks had strong intensity and narrow width indicating superior crystalline quality. Shifts in the XRD peaks occurred compared to the peak of the un-doped Yb_2O_3 sample depending on dopant rate. When Tb dopant element entered the Yb_2O_3, the peaks shifted to lower diffraction angles (inset Fig 1.) and Yb_2O_3 host expanded. Because Tb^{3+} ionic radius (0.0923 nm) is larger than that of Yb^{3+} (0.0858 nm) [15, 16]. This expansion in the structure was confirmed by the calculated lattice parameter values.

For the C-W and W-H calculations, the plots of (a) versus $f(\theta^{hkl})$ and ($\beta_{hkl}\cos\theta$) versus ($4\sin\theta$) for them are given in Fig 2.

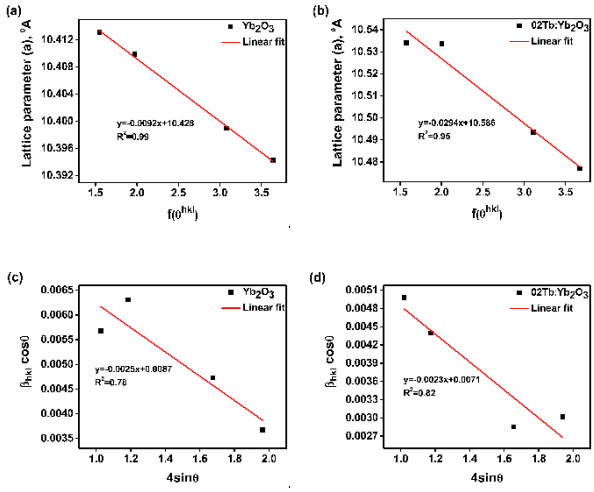

Figure 2 (a,b) C-W plots and (c,d) W-H plots of Yb_2O_3 and 02Tb:Yb_2O_3 samples

For example, according to the C–W plots of Yb_2O_3 and 02Tb:Yb_2O_3 samples the lattice parameters were 10.428 Å (R^2=99) and 10.586 Å (R^2=95), respectively. According to the W-H plots of Yb_2O_3 and 02Tb:Yb_2O_3 samples the CS values were 16 nm (R^2=78) and 19 nm (R^2=82), respectively. LP and CS values of all the particles are given in Table 2.

Table 2 Microstructural parameters of all particles.

Sample code	Lattice parameter (a/nm)	Crystallite size (nm)	Lattice strain (Ɛ)	Dislocation density (δ/nm^{-2})
Yb_2O_3	1.0428	16	-0.0025	0.00391
02Tb:Yb_2O_3	1.0586	19	-0.0023	0.00277
04Tb:Yb_2O_3	1.0590	21	-0.0016	0.00227
06Tb:Yb_2O_3	1.0593	25	-0.0011	0.00160
08Tb:Yb_2O_3	1.0596	23	-0.0014	0.00189

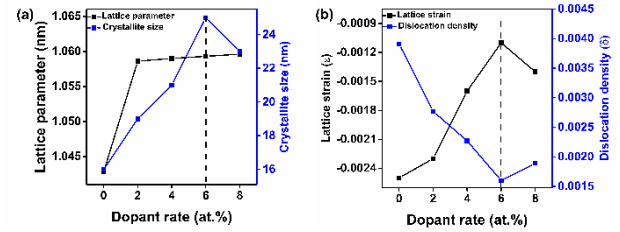

Figure 3 (a) Crystallite size and lattice parameter and (b) lattice strain and dislocation density as a function of dopant rate.

It was determined that the dopant rate enlarged the crystallites up to 6 at.%, which indicates a positive correlation between crystallite size and lattice parameter (Fig 3a). According to the dislocation density and lattice strain values, there was an improvement in crystallinity due to the reduction of crystal defects with doping. The 06Tb:Yb_2O_3 sample exhibited minimum lattice strain and dislocation density values.

3.2. Photoluminescence Analysis

The excitation spectra (Fig.4) showed the maximum excitation peak was centred at 254 nm which is belonging to 4f – 5d transition of Tb^{3+}. Thus, Un-doped and Tb doped Yb_2O_3 phosphor particles were excited by 254 nm source (inset in Fig. 4) and resulting PL emission spectra were recorded ranging from 300 nm to 800 nm. While the un-doped Yb_2O_3 particles exhibited no emission in the visible region, the Tb doped particles exhibited green emission. In addition, the PL intensity increased with the increase in the dopant rate up to 6 at. % due to the abundance of luminescence centres. Since increasing crystallite size and decreasing dislocation density improved the crystallinity, an increase in the PL emission intensity was accordingly observed. Above this dopant rate value, it was observed that the crystal defects / dislocation density values increased and the PL intensity decreased which indicates the concentration quenching of the luminescence. In the literature, Tb doped oxide particles exhibited multiple number of emission peaks. Additionally, the strongest emission peak reported to be at around 545 nm, accompanied by a low intensity emission at around 500 nm [17-22]. Contrary to the literature, the emission spectra of all the

Yb_2O_3:Tb particles were located at 506 nm associated to $^5D_4 - {}^7F_6$ transition (green emission).

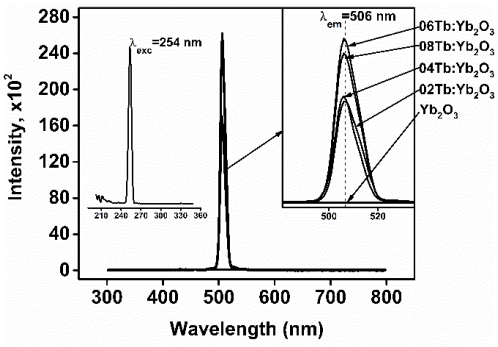

Figure 4 Excitation and emission spectra of all the particles

The PL intensity at 506 nm in emission spectra gradually increased with increasing CS and dopant rate, as shown in Fig. 4a and 4b, indicating the strong effect of the CS and the dopant rate. It was shown that the PL intensity of the Tb doped particles had a linear relationship with the CS values, indicating the improving in crystallinity (Fig. 4a). It was observed that 02Tb:Yb_2O_3 sample had the lowest PL emission intensity whereas 06Tb:Yb_2O_3 sample exhibited the highest PL emission intensity. The emission intensity value decreased for 08Tb:Yb_2O_3 sample. These results clearly show that the optimum Tb ion rate is 6 at.% for the highest PL emission intensity (Fig. 4b).. Additionally, the dopant rate had a greater significance on the PL intensity than crystallite size.

4. CONCLUSIONS

In this study, Yb_2O_3:Tb^{3+} particles having bixbyite-type cubic structure were successfully synthesized by precipitation method.

LP and CS values were in the range of 10.428 – 10.596 Å and 16 – 25 nm, respectively. Doping Tb into the Yb_2O_3 crystal increased both LP and CS values which in return decreased the dislocation density up to 6 at. % dopant rate. Further doping, started to increase lattice imperfections.

PL emission peak of all phosphor particles were centred at 506 nm corresponding to $^5D_4 - {}^7F_6$ transition (green emission). It was found that the optimum Tb dopant rate was 6 at.% due to both increasing luminescence centres and improved crystallinity, resulting in the highest PL emission intensity. However, a decrease was also observed in PL intensity above 6 at. % due to the concentration quenching.

The CS and dopant rate affected the PL intensity but, the dopant rate was more significance.

The Declaration of Conflict of Interest/ Common Interest

No conflict of interest or common interest has been declared by the author.

REFERENCES

[1] Kumar, S., Chaudhary, S., Chaudhary, G.R. 2020. Modulating physicochemical properties in Gd^{3+}@Yb_2O_3 nanospheres for efficient electrochemical monitoring of H_2O_2. *Materials Science and Engineering C*, 114, 111059.

[2] Yang, J., Shen, J., Huang, Q., Guan, Y., Miao, J. 2018. Hydrothermal synthesis and photoluminescence of host sensitized Yb_2O_3: Ho^{3+} nanorods. *Materials Research Express*, 6, 1.

[3] Henriques, M.S., Ferreiraac, A.C., Cruza, A., Ferreiraa, L.M., Brancoa, J.B., Brazdab, P., Jurekb, K., Storad, T., Gonçalvesa, A.P. 2015. Preparation of Yb_2O_3 submicron and nano materials via electrospinning. *Ceramics International*, 41, 10795–10802.

[4] Sohn, Y. 2018. Yb_2O_3 nanowires, nanorods and nano-square plates. *Ceramics International*, 44, 3341–3347.

[5] Unal, F., Kaya, F. 2020. Modelling of relation between synthesis parameters and average crystallite size of Yb_2O_3 nanoparticles using Box-Behnken design. *Ceramics International*, 46, 26800–26808.

[6] Suo, H., Guo, C., Li, L. 2015. Host sensitized spherical up-conversion

phosphor $Yb_2O_3:Er^{3+}$. *Ceramics International*, 41, 7017–7020.

[7] Zheng, Y., Lü, Q., Wang, J., Zhang, G., Gao, Y., Liu, Z. 2014. Emission behaviors of Yb_2O_3 nanoparticles pumped by 980 nm laser at different power densities. *Optics & Laser Technology*, 63, 39–44.

[8] Titov, A.A., Sokolova, N.P., Vorob'eva, M.V., Opolchenova, N.L., Eremenko, Z.V., Stepareva, N.N. 2009. Synthesis and microstructure of nanocrystalline Yb_2O_3 powders. *Inorganic Materials*, 45, 884–888.

[9] Wang, X., Li, Y., Zhou, Y., He, Y. 2019. Application of a novel endocrine disruptor bisphenol A electrochemical sensor based on analogous heterostructure characteristics of La-doped Yb_2O_3 nanomaterials. *Analytical Methods*, 11, 5613–5622.

[10] Liu, Z., Li, Z., Liu, J., Gu, S., Yuan, Q., Ren, J., Qu, X. 2012. Long-circulating Er^{3+}-doped Yb_2O_3 up-conversion nanoparticle as an in vivo X-Ray CT imaging contrast agent. *Biomaterials*, 33, 6748–6757.

[11] Qian, C., Zeng, T., Liu, H. 2013. Synthesis and downconversion emission property of Yb_2O_3: Eu^{3+} nanosheets and nanotubes. *Advances in Condensed Matter Physics*, 519869.

[12] Yuan, F., Wang, J., Miao, H., Guo, C., Wang, W.G. 2012. Investigation of the crystal structure and ionic conductivity in the ternary system $(Yb_2O_3)_x$–$(Sc_2O_3)_{(0.11-x)}$–$(ZrO_2)_{0.89}$ (x=0–0.11). *Journal of Alloys and Compounds*, 549, 200–205.

[13] Chaudhary, S., Kumar, S., Chaudhary, G.R. 2019. Tuning of structural, optical and toxicological properties of Gd^{3+} doped Yb_2O_3 nanoparticles. *Ceramics International*, 45, 19307–19315.

[14] Emil, E., Gürmen, S. 2020. A straightforward approach for the synthesis of nanostructured Y_2O_3 particles: Synthesis, morphology, microstructure and crystal imperfection. *Physica E: Low-dimensional Systems and Nanostructures*, 115, 113668.

[15] Li, X., Yang, Z., Guan, L., Guo, J., Wang, Y., Guo, Q. 2009. Synthesis and luminescent properties of $CaMoO_4:Tb^{3+}$, R+ (Li+, Na+, K^+). *Journal of Alloys and Compounds*, 478, 684–686.

[16] Tsuboi, T., Kaczmarek, S.M., Boulon, G. 2004. Spectral properties of Yb^{3+} ions in $LiNbO_3$ single crystals: Influences of other rare-earth ions, OH^- ions, and γ-irradiation. *Journal of Alloys and Compounds*, 380, 196–200.

[17] Kumamoto, N., Nakauchi, D., Kato, T., Okada, G., Kawaguchi, N., Yanagida, T. 2017. Photoluminescence, scintillation and thermally-stimulated luminescence properties of Tb-doped $12CaO{\cdot}7Al_2O_3$ single crystals grown by FZ method. *Journal of Rare Earths*, 35, 957–963.

[18] Sotiriou, G.A., Franco, D., Poulikakos, D., Ferrari, A. 2012. Optically Stable Biocompatible Flame-Made SiO_2-Coated $Y_2O_3:Tb^{3+}$ Nanophosphors for Cell Imaging. *ACS Nano*, 6, 3888–3897.

[19] Gupta, A., Brahme, N., Bisen, D.P. 2014. Electroluminescence and photoluminescence of rare earth (Eu , Tb) doped Y_2O_3 nanophosphor. *Journal of Luminescence*, 155, 112–118.

[20] An, T., Benalloul, P., Barthou, C., Giang, L.T., Vu, N., Minh, L. 2007. Luminescence, energy transfer, and upconversion mechanisms of Y_2O_3 nanomaterials doped with Eu^{3+}, Tb^{3+}, Tm^{3+}, Er^{3+}, and Yb^{3+} ions. *Journal of Nanomaterials*, 48247.

[21] Muenchausen, R.E., Jacobsohn, L.G., Bennett, B.L., McKigney, E.A., Smith, J.F., Valdez, J.A., Cooke, D.W. 2007. Effects of Tb doping on the photoluminescence of Y_2O_3:Tb nanophosphors. *Journal of Luminescence*, 126, 838–842.

[22] Tu, D., Liang, Y., Liu, R., Li, D. 2011. Eu/Tb ions co-doped white light luminescence Y_2O_3 phosphors. *Journal of Luminescence*, 131, 2569–2573.